Nehorai, A. & Paldi, E. “Electromagnetic Vector-Sensor Array Processing”
Digital Signal Processing Handbook
Ed. Vijay K. Madisetti and Douglas B. Williams
Boca Raton: CRC Press LLC, 1999

65

Electromagnetic Vector-Sensor Array Processing[1]

Arye Nehorai
The University of Illinois at Chicago

Eytan Paldi
Haifa, Israel

Dedicated to the memory of our physics teacher, Isaac Paldi

65.1 Introduction

This article (see also [1, 2]) considers new methods for multiple electromagnetic source localization using sensors whose output is a *vector* corresponding to the complete electric and magnetic fields at the sensor. These sensors, which will be called *vector sensors*, can consist for example of two orthogonal triads of scalar sensors that measure the electric and magnetic field components. Our approach is in contrast to other articles in this chapter that employ sensor arrays in which the output of each sensor is a scalar corresponding, for example, to a scalar function of the electric field. The main advantage of the vector sensors is that they make use of all available electromagnetic information and hence should outperform the scalar sensor arrays in accuracy of direction of arrival (DOA) estimation. Vector sensors should also allow the use of smaller array apertures while improving performance.

[1] This work was supported by the U.S. Air Force Office of Scientific Research under Grant no. F49620-97-1-0481, the Office of Naval Research under Grant no. N00014-96-1-1078, the National Science Foundation under Grant no. MIP-9615590, and the HTI Fellowship.

(Note that we use the term "vector sensor" for a device that measures a complete physical vector quantity.)

Section 65.2 derives the measurement model. The electromagnetic sources considered can originate from two types of transmissions: (1) Single signal transmission (SST), in which a single signal message is transmitted, and (2) dual signal transmission (DST), in which two separate signal messages are transmitted simultaneously (from the same source), see for example [3, 4]. The interest in DST is due to the fact that it makes full use of the two spatial degrees of freedom present in a transverse electromagnetic plane wave. This is particularly important in the wake of increasing demand for economical spectrum usage by existing and emerging modern communication technologies.

Section 65.3 analyzes the minimum attainable variance of unbiased DOA estimators for a general vector sensor array model and multi-electromagnetic sources that are assumed to be stochastic and stationary. A compact expression for the corresponding Cramér-Rao bound (CRB) on the DOA estimation error that extends previous results for the scalar sensor array case in [5] (see also [6]) is presented.

A significant property of the vector sensors is that they enable DOA (azimuth and elevation) estimation of an electromagnetic source with a *single* vector sensor and a single snapshot. This result is explicitly shown by using the CRB expression for this problem in Section 65.4. A bound on the associated normalized mean-square angular error (MSAE, to be defined later) which is invariant to the reference coordinate system is used for an in-depth performance study. Compact expressions for this MSAE bound provide physical insight into the SST and DST source localization problems with a single vector sensor.

The CRB matrix for an SST source in the sensor coordinate frame exhibits some nonintrinsic singularities (i.e., singularities that are not inherent in the physical model while being dependent on the choice of the reference coordinate system) and has complicated entry expressions. Therefore, we introduce a new vector angular error defined in terms of the incoming wave frame. A bound on the normalized asymptotic covariance of the vector angular error (CVAE) is derived. The relationship between the CVAE and MSAE and their bounds is presented. The CVAE matrix bound for the SST source case is shown to be diagonal, easy to interpret, and to have only intrinsic singularities.

We propose a simple algorithm for estimating the source DOA with a single vector sensor, motivated by the Poynting vector. The algorithm is applicable to various types of sources (e.g., wide-band and non-Gaussian); it does not require a minimization of a cost function and can be applied in real time. Statistical performance analysis evaluates the variance of the estimator under mild assumptions and compares it with the MSAE lower bound.

Section 65.5 extends these results to the multi-source multi-vector sensor case, with special attention to the two-source single-vector sensor case. Section 65.6 summarizes the main results and gives some ideas of possible extensions.

The main difference between the topics of this article and other articles on source direction estimation is in our use of vector sensors with *complete* electric and magnetic data. Most papers have dealt with scalar sensors. Other papers that considered estimation of the polarization state and source direction are [7]–[12]. Reference [7] discussed the use of subspace methods to solve this problem using diversely polarized electric sensors. References [8]–[10] devised algorithms for arrays with two dimensional electric measurements. Reference [11] provided performance analysis for arrays with two types of electric sensor polarizations (diversely polarized). An earlier reference, [12], proposed an estimation method using a three-dimensional vector sensor and implemented it with magnetic sensors. All these references used only part of the electromagnetic information at the sensors, thereby reducing the observability of DOAs. In most of them, time delays between distributed sensors played an essential role in the estimation process.

For a plane wave (typically associated with a single source in the far-field) the magnitude of the electric and magnetic fields can be found from each other. Hence, it may be felt that one (complete) field is deducible from the other. However, this is not true when the source direction is unknown.

Additionally, the electric and magnetic fields are orthogonal to each other and to the source DOA vector, hence measuring both fields increases significantly the accuracy of the source DOA estimation. This is true in particular for an incoming wave which is nearly linearly polarized, as will be explicitly shown by the CRB (see Table 65.1).

The use of the complete electromagnetic vector data enables source parameter estimation with a single sensor (even with a single snapshot) where time delays are not used at all. In fact, this is shown to be possible for at least two sources. As a result, the derived CRB expressions for this problem are applicable to wide-band sources. The source DOA parameters considered include azimuth and elevation. This section also considers direction estimation to DST sources, as well as the CRB on wave ellipticity and orientation angles (to be defined later) for SST sources using vector sensors, which were first presented in [1, 2]. This is true also for the MSAE and CVAE quality measures and the associated bounds. Their application is not limited to electromagnetic vector sensor processing.

We comment that electromagnetic vector sensors as measuring devices are commercially available and actively researched. EMC Baden Ltd. in Baden, Switzerland, is a company that manufactures them for signals in the 75 Hz to 30 MHz frequency range, and Flam and Russell, Inc. in Horsham, Pennsylvania, makes them for the 2 to 30 MHz frequency band. Lincoln Labs at MIT has performed some preliminary localization tests with vector sensors [13]. Some examples of recent research on sensor development are [14] and [15].

Following the recent impressive progress in the performance of DSP processors, there is a trend to fuse as much data as possible using smart sensors. Vector sensors, which belong to this category of sensors, are expected to find larger use and provide important contribution in improving the performance of DSP in the near future.

65.2 The Measurement Model

This section presents the measurement model for the estimation problems that are considered in the latter parts of the article.

65.2.1 Single-Source Single-Vector Sensor Model

Basic Assumptions

Throughout the article it will be assumed that the wave is traveling in a nonconductive, homogeneous, and isotropic medium. Additionally, the following will be assumed:

A1: Plane wave at the sensor: This is equivalent to a far-field assumption (or maximum wave-length much smaller than the source to sensor distance), a point source assumption (i.e., the source size is much smaller than the source to sensor distance) and a point-like sensor (i.e., the sensor's dimensions are small compared to the minimum wave-length).

A2: Band-limited spectrum: The signal has a spectrum including only frequencies ω satisfying $\omega_{\min} \leq |\omega| \leq \omega_{\max}$ where $0 < \omega_{\min} < \omega_{\max} < \infty$. This assumption is satisfied in practice. The lower and upper limits on ω are also needed, respectively, for the far-field and point-like sensor assumptions.

Let $\mathcal{E}(t)$ and $\mathcal{H}(t)$ be the vector phasor representations (or complex envelopes, see e.g., [16, 17] and [1, Appendix A]) of the electric and magnetic fields at the sensor. Also, let $\boldsymbol{u}$ be the unit vector at the sensor pointing towards the source, i.e.,

$$\boldsymbol{u} = \begin{bmatrix} \cos\theta_1 \cos\theta_2 \\ \sin\theta_1 \cos\theta_2 \\ \sin\theta_2 \end{bmatrix} \tag{65.1}$$

where θ_1 and θ_2 denote, respectively, the azimuth and elevation angles of $\boldsymbol{u}$, see Fig. 65.1. Thus, $\theta_1 \in [0, 2\pi)$ and $|\theta_2| \leq \pi/2$.

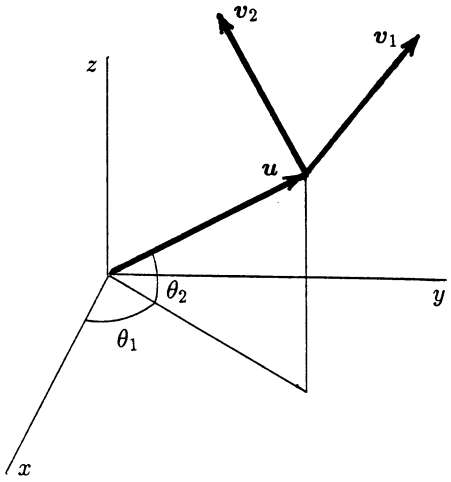

FIGURE 65.1: The orthonormal vector triad ($\boldsymbol{u}$, $\boldsymbol{v}_1$, $\boldsymbol{v}_2$).

In [1, Appendix A] it is shown that for plane waves Maxwell's equations can be reduced to an equivalent set of two equations without any loss of information. Under the additional assumption of a band-limited signal, these two equations can be written in terms of phasors. The results are summarized in the following theorem.

THEOREM 65.1 *Under assumption A1, Maxwell's equations can be reduced to an equivalent set of two equations. With the additional band-limited spectrum assumption A2, they can be written as:*

$$\boldsymbol{u} \times \mathcal{E}(t) = -\eta \mathcal{H}(t) \tag{65.2a}$$

$$\boldsymbol{u} \cdot \mathcal{E}(t) = 0 \tag{65.2b}$$

where η is the intrinsic impedance of the medium and "$\times$" and "$\cdot$" are the cross and inner products of $\mathbb{R}^3$ applied to vectors in $\mathbb{C}^3$. (That is, if $\boldsymbol{v}, \boldsymbol{w} \in \mathbb{C}^3$ then $\boldsymbol{v} \cdot \boldsymbol{w} = \sum_i v_i w_i$. This is different than the usual inner product of $\mathbb{C}^3$).

PROOF 65.1 See [1, Appendix A]. (Note that $\boldsymbol{u} = -\boldsymbol{\kappa}$ where $\boldsymbol{\kappa}$ is the unit vector in the direction of the wave propagation).

Thus, under the plane and band-limited wave assumptions, the vector phasor equations (65.2) provide all the information contained in the original Maxwell equations. This result will be used in the following to construct measurement models in which the Maxwell equations are incorporated entirely.

The Measurement Model

Suppose that a vector sensor measures all six components of the electric and magnetic fields. (It is assumed that the sensor does not influence the electric and magnetic fields). The measurement model is based on the phasor representation of the measured electromagnetic data (with respect to a reference frame) at the sensor. Let $\boldsymbol{y}_E(t)$ be the measured electric field phasor vector at the sensor at time t and $\boldsymbol{e}_E(t)$ its noise component. Then the electric part of the measurement will be

$$\boldsymbol{y}_E(t) = \mathcal{E}(t) + \boldsymbol{e}_E(t) \tag{65.3}$$

Similarly, from Eq. (65.2a), after appropriate scaling, the magnetic part of the measurement will be taken as

$$\boldsymbol{y}_H(t) = \boldsymbol{u} \times \mathcal{E}(t) + \boldsymbol{e}_H(t) \tag{65.4}$$

In addition to Eq. (65.3) and (65.4), we have the constraint (65.2b).

Define the matrix cross product operator that maps a vector $\boldsymbol{v} \in \mathbb{R}^{3\times 1}$ to $(\boldsymbol{u} \times \boldsymbol{v}) \in \mathbb{R}^{3\times 1}$ by

$$(\boldsymbol{u}\times) \triangleq \begin{bmatrix} 0 & -u_z & u_y \\ u_z & 0 & -u_x \\ -u_y & u_x & 0 \end{bmatrix} \tag{65.5}$$

where u_x, u_y, u_z are the x, y, z components of the vector $\boldsymbol{u}$. With this definition, Eqs. (65.3) and (65.4) can be combined to

$$\begin{bmatrix} \boldsymbol{y}_E(t) \\ \boldsymbol{y}_H(t) \end{bmatrix} = \begin{bmatrix} I_3 \\ (\boldsymbol{u}\times) \end{bmatrix} \mathcal{E}(t) + \begin{bmatrix} \boldsymbol{e}_E(t) \\ \boldsymbol{e}_H(t) \end{bmatrix} \tag{65.6}$$

where I_3 denotes the 3×3 identity matrix. For notational convenience the dimension subscript of the identity matrix will be omitted whenever its value is clear from the context.

The constraint (65.2b) implies that the electric phasor $\mathcal{E}(t)$ can be written

$$\mathcal{E}(t) = V\boldsymbol{\xi}(t) \tag{65.7}$$

where V is a 3×2 matrix whose columns span the orthogonal complement of $\boldsymbol{u}$ and $\boldsymbol{\xi}(t) \in \mathbb{C}^{2\times 1}$. It is easy to check that the matrix

$$V = \begin{bmatrix} -\sin\theta_1 & -\cos\theta_1 \sin\theta_2 \\ \cos\theta_1 & -\sin\theta_1 \sin\theta_2 \\ 0 & \cos\theta_2 \end{bmatrix} \tag{65.8}$$

whose columns are orthonormal, satisfies this requirement. We note that since $\|\boldsymbol{u}\|^2 = 1$ the columns of V, denoted by $\boldsymbol{v}_1$ and $\boldsymbol{v}_2$, can be constructed, for example, from the partial derivatives of $\boldsymbol{u}$ with respect to θ_1 and θ_2 and post-normalization when needed. Thus,

$$\boldsymbol{v}_1 = \frac{1}{\cos\theta_2}\frac{\partial \boldsymbol{u}}{\partial \theta_1} \tag{65.9a}$$

$$\boldsymbol{v}_2 = \boldsymbol{u} \times \boldsymbol{v}_1 = \frac{\partial \boldsymbol{u}}{\partial \theta_2} \tag{65.9b}$$

and $(\boldsymbol{u}, \boldsymbol{v}_1, \boldsymbol{v}_2)$ is a right orthonormal triad, see Fig. 65.1. (Observe that the two coordinate systems shown in the figure actually have the same origin). The signal $\boldsymbol{\xi}(t)$ fully determines the components of $\mathcal{E}(t)$ in the plane where it lies, namely the plane orthogonal to $\boldsymbol{u}$ spanned by $\boldsymbol{v}_1, \boldsymbol{v}_2$. This implies that there are two degrees of freedom present in the spatial domain (or the wave's plane), or two independent signals can be transmitted simultaneously.

Combining Eq. (65.6) and Eq. (65.7) we now have

$$\begin{bmatrix} \boldsymbol{y}_E(t) \\ \boldsymbol{y}_H(t) \end{bmatrix} = \begin{bmatrix} I \\ (\boldsymbol{u}\times) \end{bmatrix} V\boldsymbol{\xi}(t) + \begin{bmatrix} \boldsymbol{e}_E(t) \\ \boldsymbol{e}_H(t) \end{bmatrix} \tag{65.10}$$

This system is equivalent to Eq. (65.6) with Eq. (65.2b).

The measured signals in the sensor reference frame can be further related to the original source signal at the transmitter using the following lemma.

LEMMA 65.1 Every vector $\boldsymbol{\xi} = [\xi_1, \xi_2]^T \in \mathbb{C}^{2\times 1}$ has the representation

$$\boldsymbol{\xi} = \|\boldsymbol{\xi}\| e^{i\varphi} Q\boldsymbol{w} \tag{65.11}$$

where

$$Q = \begin{bmatrix} \cos\theta_3 & \sin\theta_3 \\ -\sin\theta_3 & \cos\theta_3 \end{bmatrix} \tag{65.12a}$$

$$\boldsymbol{w} = \begin{bmatrix} \cos\theta_4 \\ i\sin\theta_4 \end{bmatrix} \tag{65.12b}$$

and where $\varphi \in (-\pi, \pi]$, $\theta_3 \in (-\pi/2, \pi/2]$, $\theta_4 \in [-\pi/4, \pi/4]$. Moreover, $\|\boldsymbol{\xi}\|, \varphi, \theta_3, \theta_4$ in Eq. (65.11) are uniquely determined if and only if $\xi_1^2 + \xi_2^2 \neq 0$.

PROOF 65.2 See [1, Appendix B].

The equality $\xi_1^2 + \xi_2^2 = 0$ holds if and only if $|\theta_4| = \pi/4$, corresponding to circular polarization (defined below). Hence, from Lemma 65.1 the representation (65.11), (65.12) is not unique in this case as should be expected, since the orientation angle θ_3 is ambiguous. It should be noted that the representation (65.11), (65.12) is known and was used (see, e.g., [18]) without a proof. However, Lemma 65.1 of existence and uniqueness appears to be new. The existence and uniqueness properties are important to guarantee identifiability of parameters.

The physical interpretations of the quantities in the representation (65.11), (65.12) are as follows.

$\|\boldsymbol{\xi}\| e^{i\varphi}$: Complex envelope of the source signal (including amplitude and phase).

$\boldsymbol{w}$: Normalized overall transfer vector of the source's antenna and medium, i.e., from the source complex envelope signal to the principal axes of the received electric wave.

Q: A rotation matrix that performs the rotation from the principal axes of the incoming electric wave to the $(\boldsymbol{v}_1, \boldsymbol{v}_2)$ coordinates.

Let ω_c be the reference frequency of the signal phasor representation, see [1, Appendix A]. In the narrow-band SST case, the incoming electric wave signal $\mathrm{Re}\{e^{i\omega_c t}\|\boldsymbol{\xi}(t)\|e^{i\varphi(t)}Q\boldsymbol{w}\}$ moves on a quasi-stationary ellipse whose semi-major and semi-minor axes' lengths are proportional, respectively, to $\cos\theta_4$ and $\sin\theta_4$, see Fig. 65.2 and [19]. The ellipse's eccentricity is thus determined by the magnitude of θ_4. The sign of θ_4 determines the spin sign or direction. More precisely, a positive (negative) θ_4 corresponds to a positive (negative) spin with right-(left) handed rotation with respect to the wave propagation vector $\boldsymbol{\kappa} = -\boldsymbol{u}$. As shown in Fig. 65.2, θ_3 is the rotation angle between the $(\boldsymbol{v}_1, \boldsymbol{v}_2)$ coordinates and the electric ellipse axes $(\widetilde{\boldsymbol{v}}_1, \widetilde{\boldsymbol{v}}_2)$. The angles θ_3 and θ_4 will be referred to, respectively,

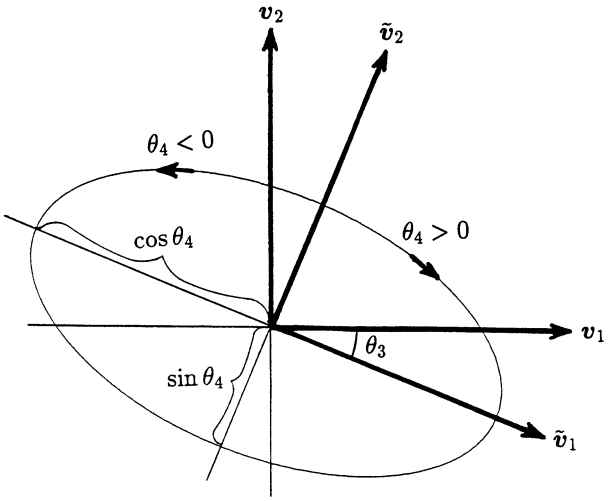

FIGURE 65.2: The electric polarization ellipse.

as the orientation and ellipticity angles of the received electric wave ellipse. In addition to the electric ellipse, there is also a similar but perpendicular magnetic ellipse.

It should be noted that if the transfer matrix from the source to the sensor is time invariant, then so are θ_3 and θ_4.

The signal $\boldsymbol{\xi}(t)$ can carry information coded in various forms. In the following we discuss briefly both existing forms and some motivated by the above representation.

Single Signal Transmission (SST) Model

Suppose that a single modulated signal is transmitted. Then, using Eq. (65.11), this is a special case of Eq. (65.10) with

$$\boldsymbol{\xi}(t) = Q\boldsymbol{w}s(t) \tag{65.13}$$

where $s(t)$ denotes the complex envelope of the (scalar) transmitted signal. Thus, the measurement model is

$$\begin{bmatrix} \boldsymbol{y}_E(t) \\ \boldsymbol{y}_H(t) \end{bmatrix} = \begin{bmatrix} I \\ (\boldsymbol{u}\times) \end{bmatrix} VQ\boldsymbol{w}s(t) + \begin{bmatrix} \boldsymbol{e}_E(t) \\ \boldsymbol{e}_H(t) \end{bmatrix} \tag{65.14}$$

Special cases of this transmission are linear polarization with $\theta_4 = 0$ and circular polarization with $|\theta_4| = \pi/4$.

Recall that since there are two spatial degrees of freedom in a transverse electromagnetic plane wave, one could, in principle, transmit two separate signals simultaneously. Thus, the SST method does not make full use of the two spatial degrees of freedom present in a transverse electromagnetic plane wave.

Dual Signal Transmission (DST) Models

Methods of transmission in which two separate signals are transmitted simultaneously from the same source will be called *dual signal transmissions*. Various DST forms exist, and all of them can be modeled by Eq. (65.10) with $\boldsymbol{\xi}(t)$ being a linear transformation of the two-dimensional source signal vector.

One DST form uses two linearly polarized signals that are spatially and temporally orthogonal with an amplitude or phase modulation (see e.g., [3, 4]). This is a special case of Eq. (65.10), where

the signal $\boldsymbol{\xi}(t)$ is written in the form

$$\boldsymbol{\xi}(t) = Q \begin{bmatrix} s_1(t) \\ is_2(t) \end{bmatrix} \tag{65.15}$$

where $s_1(t)$ and $s_2(t)$ represent the complex envelopes of the transmitted signals. To guarantee unique decoding of the two signals (when θ_3 is unknown) using Lemma 65.1, they have to satisfy $s_1(t) \neq 0$, $s_2(t)/s_1(t) \in (-1, 1)$. (Practically this can be achieved by using a proper electronic antenna adapter that yields a desirable overall transfer matrix.)

Another DST form uses two circularly polarized signals with opposite spins. In this case

$$\boldsymbol{\xi}(t) = Q[\boldsymbol{w}\widetilde{s}_1(t) + \overline{\boldsymbol{w}}\widetilde{s}_2(t)] \tag{65.16a}$$

$$\boldsymbol{w} = (1/\sqrt{2})[1,\ i]^T \tag{65.16b}$$

where $\overline{\boldsymbol{w}}$ denotes the complex conjugate of $\boldsymbol{w}$. The signals $\widetilde{s}_1(t), \widetilde{s}_2(t)$ represent the complex envelopes of the transmitted signals. The first term on the r.h.s. of Eqs. (65.16) corresponds to a signal with positive spin and circular polarization ($\theta_4 = \pi/4$), while the second term corresponds to a signal with negative spin and circular polarization ($\theta_4 = -\pi/4$). The uniqueness of Eqs. (65.16) is guaranteed without the conditions needed for the uniqueness of Eq. (65.15).

The above-mentioned DST models can be applied to communication problems. Assuming that $\boldsymbol{u}$ is given, it is possible to measure the signal $\boldsymbol{\xi}(t)$ and recover the original messages as follows. For Eq. (65.15), an existing method resolves the two messages using mechanical orientation of the receiver's antenna (see, e.g., [4]). Alternatively, this can be done electronically using the representation of Lemma 65.1, without the need to know the orientation angle. For Eqs. (65.16), note that $\boldsymbol{\xi}(t) = \boldsymbol{w}e^{i\theta_3}\widetilde{s}_1(t) + \overline{\boldsymbol{w}}e^{-i\theta_3}\widetilde{s}_2(t)$, which implies the uniqueness of Eqs. (65.16) and indicates that the orientation angle has been converted into a phase angle whose sign depends on the spin sign. The original signals can be directly recovered from $\boldsymbol{\xi}(t)$ up to an additive constant phase without knowledge of the orientation angle. In some cases, it is of interest to estimate the orientation angle. Let W be a matrix whose columns are $\boldsymbol{w}, \overline{\boldsymbol{w}}$. For Eqs. (65.16) this can be done using equal calibrating signals and then premultiplying the measurement by W^{-1} and measuring the phase difference between the two components of the result. This can also be used for real time estimation of the angular velocity $d\theta_3/dt$.

In general it can be stated that the advantage of the DST method is that it makes full use of the spatial degrees of freedom of transmission. However, the above DST methods need the knowledge of $\boldsymbol{u}$ and, in addition, may suffer from possible cross polarizations (see, e.g., [3]), multipath effects, and other unknown distortions from the source to the sensor.

The use of the proposed vector sensor can motivate the design of new improved transmission forms. Here we suggest a new dual signal transmission method that uses on line electronic calibration in order to resolve the above problems. Similar to the previous methods it also makes full use of the spatial degrees of freedom in the system. However, it overcomes the need to know $\boldsymbol{u}$ and the overall transfer matrix from source to sensor.

Suppose the transmitted signal is $z(t) \in \mathbb{C}^{2\times 1}$ (this signal is as it appears before reaching the source's antenna). The measured signal is

$$\begin{bmatrix} \boldsymbol{y}_E(t) \\ \boldsymbol{y}_H(t) \end{bmatrix} = C(t)z(t) + \begin{bmatrix} \boldsymbol{e}_E(t) \\ \boldsymbol{e}_H(t) \end{bmatrix} \tag{65.17}$$

where $C(t) \in \mathbb{C}^{6\times 2}$ is the unknown source to sensor transfer matrix that may be slowly varying due to, for example, the source dynamics. To facilitate the identification of $z(t)$, the transmitter can send calibrating signals, for instance, transmit $z_1(t) = [1, 0]^T$ and $z_2(t) = [0, 1]^T$ separately. Since these

inputs are in phasor form, this means that actually constant carrier waves are transmitted. Obviously, one can then estimate the columns of $C(t)$ by averaging the received signals, which can be used later for finding the original signal $\boldsymbol{z}(t)$ by using, for example, least-squares estimation. Better estimation performance can be achieved by taking into account *a priori* information about the model.

The use of vector sensors is attractive in communication systems as it doubles the channel capacity (compared with scalar sensors) by making full use of the electromagnetic wave properties. This spatial multiplexing has vast potential for performance improvement in cellular communications.

In future research it would be of interest to develop optimal coding methods (modulation forms) for maximum channel capacity while maintaining acceptable distortions of the decoded signals despite unknown varying channel characteristics. It would also be of interest to design communication systems that utilize entire arrays of vector sensors.

Observe that actually any combination of the variables $\|\boldsymbol{\xi}\|$, φ, θ_3 and θ_4 can be modulated to carry information. A binary signal can be transmitted using the spin sign of the polarization ellipse (sign of θ_4). Lemma 65.1 guarantees the identifiability of these signals from $\boldsymbol{\xi}(t)$.

65.2.2 Multi-Source Multi-Vector Sensor Model

Suppose that waves from n distant electromagnetic sources are impinging on an array of m vector sensors and that assumptions A1 and A2 hold for each source. To extend the model (65.10) to this scenario we need the following additional assumptions, which imply that A1, A2 hold uniformly on the array:

A3: Plane wave across the array: In addition to A1, for each source the array size d_A has to be much smaller than the source to array distance, so that the vector $\boldsymbol{u}$ is approximately independent of the individual sensor positions.

A4: Narrow-band signal assumption: The maximum frequency of $\mathcal{E}(t)$, denoted by ω_m, satisfies $\omega_m d_A/c \ll 1$, where c is the velocity of wave propagation (i.e., the minimum modulating wave-length is much larger than the array size). This implies that $\mathcal{E}(t-\tau) \simeq \mathcal{E}(t)$ for all differential delays τ of the source signals between the sensors.

Note that (under the assumption $\omega_m < \omega_c$) since $\omega_m = \max\{|\omega_{\min} - \omega_c|, |\omega_{\max} - \omega_c|\}$, it follows that A4 is satisfied if $(\omega_{\max} - \omega_{\min})d_A/2c \ll 1$ and ω_c is chosen to be close enough to $(\omega_{\max} + \omega_{\min})/2$.

Let $\boldsymbol{y}_{EH}(t)$ and $\boldsymbol{e}_{EH}(t)$ be the $6m \times 1$ dimensional electromagnetic sensor phasor measurement and noise vectors,

$$\boldsymbol{y}_{EH}(t) \triangleq \left[(\boldsymbol{y}_E^{(1)}(t))^T,\ (\boldsymbol{y}_H^{(1)}(t))^T,\ \cdots,\ (\boldsymbol{y}_E^{(m)}(t))^T,\ (\boldsymbol{y}_H^{(m)}(t))^T\right]^T \tag{65.18a}$$

$$\boldsymbol{e}_{EH}(t) \triangleq \left[(\boldsymbol{e}_E^{(1)}(t))^T,\ (\boldsymbol{e}_H^{(1)}(t))^T,\ \cdots,\ (\boldsymbol{e}_E^{(m)}(t))^T,\ (\boldsymbol{e}_H^{(m)}(t))^T\right]^T \tag{65.18b}$$

where $\boldsymbol{y}_E^{(j)}(t)$ and $\boldsymbol{y}_H^{(j)}(t)$ are, respectively, the measured phasor electric and magnetic vector fields at the jth sensor and similarly for the noise components $\boldsymbol{e}_E^{(j)}(t)$ and $\boldsymbol{e}_H^{(j)}(t)$. Then, under assumptions A3 and A4 and from Eq. (65.10), we find that the array measured phasor signal can be written as

$$\boldsymbol{y}_{EH}(t) = \sum_{k=1}^{n} \boldsymbol{e}_k \otimes \begin{bmatrix} I_3 \\ (\boldsymbol{u}_k \times) \end{bmatrix} V_k \boldsymbol{\xi}_k(t) + \boldsymbol{e}_{EH}(t) \tag{65.19}$$

where $\otimes$ is the Kronecker product, $\boldsymbol{e}_k$ denotes the kth column of the matrix $E \in \mathbb{C}^{m\times n}$ whose (j,k) entry is

$$E_{jk} = e^{-i\omega_c \tau_{jk}} \tag{65.20}$$

where τ_{jk} is the differential delay of the kth source signal between the jth sensor and the origin of some fixed reference coordinate system (e.g., at one of the sensors). Thus, $\tau_{jk} = -(\boldsymbol{u}_k \cdot \boldsymbol{r}_j)/c$, where $\boldsymbol{u}_k$ is the unit vector in the direction from the array to the kth source and $\boldsymbol{r}_j$ is the position vector of the jth sensor in the reference frame. The rest of the notation in Eq. (65.19) is similar to the single source case, cf. Eqs. (65.1), (65.8), and (65.10). The vector $\boldsymbol{\xi}_k(t)$ can have either the SST or the DST form described above.

Observe that the signal manifold matrix in Eq. (65.19) can be written as the Khatri-Rao product (see, e.g., [20, 21]) of E and a second matrix whose form depends on the source transmission type (i.e., SST or DST), see also later.

65.3 Cramér-Rao Bound for a Vector Sensor Array

65.3.1 Statistical Model

Consider the problem of finding the parameter vector $\boldsymbol{\theta}$ in the following discrete-time vector sensor array model associated with n vector sources and m vector sensors:

$$\boldsymbol{y}(t) = A(\boldsymbol{\theta})\boldsymbol{x}(t) + \boldsymbol{e}(t) \qquad t = 1, 2, \ldots \tag{65.21}$$

where $\boldsymbol{y}(t) \in \mathbb{C}^{\overline{\mu}\times 1}$ are the vectors of observed sensor outputs (or snapshots), $\boldsymbol{x}(t) \in \mathbb{C}^{\overline{\nu}\times 1}$ are the unknown source signals, and $\boldsymbol{e}(t) \in \mathbb{C}^{\overline{\mu}\times 1}$ are the additive noise vectors. The transfer matrix $A(\boldsymbol{\theta}) \in \mathbb{C}^{\overline{\mu}\times\overline{\nu}}$ and the parameter vector $\boldsymbol{\theta} \in \mathbb{R}^{\overline{q}\times 1}$ are given by

$$A(\boldsymbol{\theta}) = \left[A_1(\boldsymbol{\theta}^{(1)}) \cdots A_n(\boldsymbol{\theta}^{(n)})\right] \tag{65.22a}$$

$$\boldsymbol{\theta} = \left[(\boldsymbol{\theta}^{(1)})^T, \cdots, (\boldsymbol{\theta}^{(n)})^T\right]^T \tag{65.22b}$$

where $A_k(\boldsymbol{\theta}^{(k)}) \in \mathbb{C}^{\overline{\mu}\times\nu_k}$ and the parameter vector of the kth source $\boldsymbol{\theta}^{(k)} \in \mathbb{R}^{q_k\times 1}$, thus $\overline{\nu} = \sum_{k=1}^{n} \nu_k$ and $\overline{q} = \sum_{k=1}^{n} q_k$. The following notation will also be used:

$$\boldsymbol{y}(t) = \left[(\boldsymbol{y}^{(1)}(t))^T, \cdots, (\boldsymbol{y}^{(m)}(t))^T\right]^T \tag{65.23a}$$

$$\boldsymbol{x}(t) = \left[(\boldsymbol{x}^{(1)}(t))^T, \cdots, (\boldsymbol{x}^{(n)}(t))^T\right]^T \tag{65.23b}$$

where $\boldsymbol{y}^{(j)}(t) \in \mathbb{C}^{\mu_j\times 1}$ is the vector measurement of the jth sensor, implying $\overline{\mu} = \sum_{j=1}^{m} \mu_j$, and $\boldsymbol{x}^{(k)}(t) \in \mathbb{C}^{\nu_k\times 1}$ is the vector signal of the kth source. Clearly $\overline{\mu}$ and $\overline{\nu}$ correspond, respectively, to the total number of sensor components and source signal components.

The model (65.21) generalizes the commonly used multi-scalar source multi-scalar sensor one (see, e.g., [7, 22]). It will be shown later that the electromagnetic multi-vector source multi-vector sensor data models are special cases of Eq. (65.21) with appropriate choices of matrices.

For notational simplicity, the explicit dependence on $\boldsymbol{\theta}$ and t will be occasionally omitted.

We make the following commonly used assumptions on the model (65.21):

A5: The source signal sequence $\{\boldsymbol{x}(1), \boldsymbol{x}(2), \ldots\}$ is a sample from a temporally uncorrelated stationary (complex) Gaussian process with zero mean and

$$\mathrm{E}\,\boldsymbol{x}(t)\boldsymbol{x}^*(s) = P\delta_{t,s}$$
$$\mathrm{E}\,\boldsymbol{x}(t)\boldsymbol{x}^T(s) = 0 \qquad \text{(for all } t \text{ and } s\text{)}.$$

where E is the expectation operator, the superscript "*" denotes the conjugate transpose, and $\delta_{t,s}$ is the Kronecker delta.

A6: The noise $\boldsymbol{e}(t)$ is (complex) Gaussian distributed with zero mean and

$$\mathrm{E}\,\boldsymbol{e}(t)\boldsymbol{e}^*(s) = \sigma^2 I \delta_{t,s}$$
$$\mathrm{E}\,\boldsymbol{e}(t)\boldsymbol{e}^T(s) = 0 \qquad \text{(for all } t \text{ and } s\text{)}.$$

It is also assumed that the signals $\boldsymbol{x}(t)$ and the noise $\boldsymbol{e}(s)$ are independent for all t and s.

A7: The matrix A has full rank $\overline{\nu} < \overline{\mu}$ (thus A^*A is p.d.) and a continuous Jacobian $\partial A/\partial \boldsymbol{\theta}$ in some neighborhood of the true $\boldsymbol{\theta}$. The matrix $APA^* + \sigma^2 I$ is assumed to be positive definite, which implies that the probability density functions of the model are well defined in some neighborhood of the true $\boldsymbol{\theta}$, P, σ^2. Additionally, the matrix in braces in Eq. (65.24) below is assumed to be nonsingular.

The unknown parameters in the model (65.21) include the vector $\boldsymbol{\theta}$, the signal covariance matrix P, and the noise variance σ^2. The problem of estimating $\boldsymbol{\theta}$ in (65.21) from N snapshots $\boldsymbol{y}(1), \ldots, \boldsymbol{y}(N)$ and the statistical performance of estimation methods are the main concerns of this article.

65.3.2 The Cramér-Rao Bound

Consider the estimation of $\boldsymbol{\theta}$ in the model (65.21) under the above assumptions and with $\boldsymbol{\theta}$, P, σ^2 unknown. We have the following theorem.

THEOREM 65.2 *The Cramér-Rao lower bound on the covariance matrix of any (locally) unbiased estimator of the vector $\boldsymbol{\theta}$ in the model (65.21), under assumptions A5 through A7 with $\boldsymbol{\theta}$, P, σ^2 unknown and $\nu_k = \nu$ for all k, is a positive definite matrix given by*

$$\mathrm{CRB}(\boldsymbol{\theta}) = \frac{\sigma^2}{2N}\left\{\mathrm{Re}\left[\mathrm{btr}\left(\left(\mathbf{1}\boxtimes U\right)\boxdot\left(D^*\Pi_c D\right)^{bT}\right)\right]\right\}^{-1} \tag{65.24}$$

where

$$U = P\left(A^*AP + \sigma^2 I\right)^{-1} A^*AP \tag{65.25a}$$
$$\Pi_c = I - \Pi \tag{65.25b}$$
$$\Pi = A(A^*A)^{-1}A^* \tag{65.25c}$$
$$D = \left[D_1^{(1)} \cdots D_{q_1}^{(1)} \quad \cdots \quad D_1^{(n)} \cdots D_{q_n}^{(n)}\right] \tag{65.25d}$$
$$D_\ell^{(k)} = \frac{\partial A_k}{\partial \theta_\ell^{(k)}} \tag{65.25e}$$

and where $\mathbf{1}$ denotes a $\overline{q} \times \overline{q}$ matrix with all entries equal to one, and the block trace operator btr $(\cdot)$*, the block Kronecker product $\boxtimes$, the block Schur-Hadamard product $\boxdot$, and the block transpose operator bT are as defined in the Appendix with blocks of dimensions $\nu \times \nu$, except for the matrix $\mathbf{1}$ that has blocks of dimensions $q_i \times q_j$.*

Furthermore, the CRB in Eq. (65.24) remains the same independently of whether σ^2 is known or unknown.

PROOF 65.3 See [1, Appendix C].

Theorem 65.2 can be extended to include a larger class of unknown sensor noise covariance matrices (see [1, Appendix D]).

65.4 MSAE, CVAE, and Single-Source Single-Vector Sensor Analysis

This section introduces the MSAE and CVAE quality measures and their bounds for source direction and orientation estimation in three-dimensional space. The bounds are applied to analyze the statistical performance of parameter estimation of an electromagnetic source whose covariance is unknown using a single vector sensor. Note that single vector sensor analysis is valid for *wide-band* sources, as assumptions A3 and A4 are not needed.

65.4.1 The MSAE

We define the mean-square angular error which is a quality measure that is useful for gaining physical insight into DOA (azimuth and elevation) estimation and for performance comparisons. The analysis of this subsection is not limited to electromagnetic measurements or to Gaussian data.

The angular error, say δ, corresponding to a direction error $\Delta\boldsymbol{u}$ in $\boldsymbol{u}$, can be shown to be $\delta = 2\arcsin(\|\Delta\boldsymbol{u}\|/2)$. Hence, $\delta^2 = \|\Delta\boldsymbol{u}\|^2 + O(\|\Delta\boldsymbol{u}\|^4)$. Since $\Delta\boldsymbol{u} = \left(\frac{\partial\boldsymbol{u}}{\partial\theta_1}\right)\Delta\theta_1 + \left(\frac{\partial\boldsymbol{u}}{\partial\theta_2}\right)\Delta\theta_2 + O((\Delta\theta_1)^2 + (\Delta\theta_2)^2)$ where $\Delta\theta_1$, $\Delta\theta_2$ are the errors in θ_1 and θ_2, we have

$$\delta^2 = (\cos\theta_2 \cdot \Delta\theta_1)^2 + (\Delta\theta_2)^2 + O(|\Delta\theta_1|^3 + |\Delta\theta_2|^3) \tag{65.26}$$

We introduce the following definitions.

DEFINITION 65.1 A model will be called *regular* if it satisfies any set of sufficient conditions for the CRB to hold (see, e.g., [23, 24]).

DEFINITION 65.2 The *normalized asymptotic mean-square angular error* of a direction estimator will be defined as

$$\text{MSAE} \triangleq \lim_{N\to\infty}\left\{N\,\text{E}\,(\delta^2)\right\} \tag{65.27}$$

whenever this limit exists.

DEFINITION 65.3 A direction estimator will be called *regular* if its errors satisfy $\text{E}\left[|\Delta\theta_1|^3 + |\Delta\theta_2|^3\right] = o(1/N)$, the gradient of its bias with respect to θ_1, θ_2 exists and is $o(1)$ as $N \to \infty$, and its MSAE exists. (If $|\theta_2| = \pi/2$ then θ_1 is undefined and we can use the equivalent condition $\text{E}\left[\|\Delta\boldsymbol{u}\|^3\right] = o(1/N)$).

Equation (65.26) shows that under the assumptions that the model and estimator are regular we have

$$\text{E}\,(\delta)^2 \geq [\cos^2\theta_2 \cdot \text{CRB}(\theta_1) + \text{CRB}(\theta_2)] + o(1/N) \qquad \text{as } N \to \infty \tag{65.28}$$

where $\text{CRB}(\theta_1)$ and $\text{CRB}(\theta_2)$ are, respectively, the Cramér-Rao bounds for the azimuth and elevation. Using Eq. (65.28) we have the following theorem.

THEOREM 65.3 *For a regular model MSAE of any regular direction estimator is bounded from below by*

$$\text{MSAE}_{CR} \triangleq N[\cos^2\theta_2 \cdot \text{CRB}(\theta_1) + \text{CRB}(\theta_2)] \tag{65.29}$$

Observe that MSAE_{CR} is not a function of N. Additionally, MSAE_{CR} is a tight bound if it is attained by some second order efficient regular estimator (usually the maximum likelihood (ML) estimator, see e.g., [25]). For vector sensor measurements this bound has the desirable property of being invariant to the choice of reference coordinate frame, since the information content in the data is invariant under rotational transformations. This invariance property also holds for the MSAE of an estimator if the estimate is independent of known rotational transformations of the data.

For a regular model, the bound (65.29) can be used for performance analysis of any regular direction (azimuth and elevation) finding algorithm.

It is of interest to note that the bound (65.29) actually holds for finite data, when the estimators of $\boldsymbol{u}$ are unbiased and constrained to be of unit norm, see [26].

65.4.2 DST Source Analysis

Assume that it is desired to estimate the direction to a DST source whose covariance is unknown using a vector sensor. We will first present a statistical model for this problem as a special case of Eq. (65.21) and then investigate in detail the resulting CRB and MSAE.

The measurement model for the DST case is given in Eq. (65.10). Suppose the noise vector of Eq. (65.10) is (complex) Gaussian with zero mean and the following covariances:

$$\mathrm{E}\begin{bmatrix} \boldsymbol{e}_E(t) \\ \boldsymbol{e}_H(t) \end{bmatrix}\begin{bmatrix} \boldsymbol{e}_E^*(s), & \boldsymbol{e}_H^*(s) \end{bmatrix} = \begin{bmatrix} \sigma_E^2 I_3 & 0 \\ 0 & \sigma_H^2 I_3 \end{bmatrix}\delta_{t,s}$$

$$\mathrm{E}\begin{bmatrix} \boldsymbol{e}_E(t) \\ \boldsymbol{e}_H(t) \end{bmatrix}\begin{bmatrix} \boldsymbol{e}_E^T(s), & \boldsymbol{e}_H^T(s) \end{bmatrix} = 0 \qquad (\text{for all } t \text{ and } s).$$

Our assumption that the noise components are statistically independent stems from the fact that they are created separately at *different* sensor components (even if the sensor components belong to a vector sensor). Note that under assumption A1 the measurement includes a source plane wave component and sensor self noise.

To relate the model (65.10) to (65.21), define a scaled measurement $\boldsymbol{y}(t) \triangleq \left[r\boldsymbol{y}_E^T(t),\ \boldsymbol{y}_H^T(t)\right]^T$ where $r \triangleq \sigma_H/\sigma_E$ is assumed to be known. (The results of this section actually hold also when r is unknown as is explained in [1]). The resulting scaled noise vector $\boldsymbol{e}(t) \triangleq \left[r\boldsymbol{e}_E^T(t),\ \boldsymbol{e}_H^T(t)\right]^T$ then satisfies assumption A6 with $\sigma = \sigma_H$. Assume further that the signal $\boldsymbol{\xi}(t)$ satisfies assumption A5 with $\boldsymbol{x}(t) = \boldsymbol{\xi}(t)$. Then, under these assumptions, the scaled version of the DST source (65.10) can be viewed as a special case of Eq. (65.21) with $m = n = 1$ and

$$\begin{aligned} A &= \begin{bmatrix} rV \\ (\boldsymbol{u}\times)V \end{bmatrix} \qquad \boldsymbol{x}(t) = \boldsymbol{\xi}(t) \qquad \sigma^2 = \sigma_H^2 \\ \boldsymbol{\theta} &= \begin{bmatrix} \theta_1, & \theta_2 \end{bmatrix}^T \end{aligned} \tag{65.30}$$

where the unknown parameters are $\boldsymbol{\theta}$, P, σ^2. The parameter vector of interest is $\boldsymbol{\theta}$ while P and σ^2 are the so-called nuisance parameters.

The above discussion shows that the CRB expression (65.24) is applicable to the present problem with the special choice of variables in Eq. (65.30), thus $n = 1$ and $\overline{q} = 2$. The computation of the CRB is given in [1]. The result is independent of whether r is known or unknown.

Using the CRB results of [1] we find that MSAE_{CR} for the present DST problem is

$$\mathrm{MSAE}_{CR}^D = \frac{\left(\sigma_E^2 + \sigma_H^2\right)\sigma_E^2\sigma_H^2\,\mathrm{tr}\,U}{2\left[\sigma_E^2\sigma_H^2\,(\mathrm{tr}\,U)^2 + \left(\sigma_E^2 - \sigma_H^2\right)^2\det\left(\mathrm{Re}\,U\right)\right]} \tag{65.31}$$

Observe that MSAE_{CR}^D is symmetric with respect to σ_E, σ_H, as should be expected from the Maxwell equations. MSAE_{CR}^D is not a function of θ_1, θ_2, θ_3, as should be expected since for vector sensor

measurements the MSAE bound is by definition invariant to the choice of coordinate system. Note that MSAE_{CR}^{D} is independent of whether σ_E and σ_H are known or unknown.

65.4.3 SST Source (DST Model) Analysis

Consider the MSAE for a single signal transmission source when the estimation is done under the assumption that the source is of a dual signal transmission type. In this case, the model (65.10) has to be used but with a signal in the form of (65.13). The signal covariance is then

$$P = \sigma_s^2 Q\boldsymbol{w}(Q\boldsymbol{w})^* \tag{65.32}$$

where $\sigma_s^2 = \mathrm{E}\, s^2(t)$ and Q and $\boldsymbol{w}$ are defined in Eq. (65.12). Thus, rank $P = 1$ and P has a unit norm eigenvector $Q\boldsymbol{w}$ with an eigenvalue σ_s^2.

Let

$$\sigma_{\|}^2 \triangleq \frac{\sigma_E^2 \cdot \sigma_H^2}{\sigma_E^2 + \sigma_H^2} \tag{65.33}$$

The variance $\sigma_{\|}^2$ can be viewed as an equivalent noise variance of two measurements with independent noise variances σ_E^2 and σ_H^2. Define $\varrho \triangleq \sigma_s^2/\sigma_{\|}^2$, which is an effective SNR.

Using the analysis of U in [1] and expression (65.31) we find that

$$\begin{aligned} \mathrm{MSAE}_{CR}^{S} &= \frac{(1+\varrho)(\sigma_E^2+\sigma_H^2)^2}{2\varrho^2\left[\sigma_E^2\sigma_H^2 + (\sigma_E^2-\sigma_H^2)^2 \sin^2\theta_4 \cos^2\theta_4\right]} \\ &= \frac{(1+\varrho)(1+r^2)^2}{2\varrho^2\left[r^2 + (1-r^2)^2 \sin^2\theta_4 \cos^2\theta_4\right]} \end{aligned} \tag{65.34}$$

where MSAE_{CR}^{S} denotes the MSAE_{CR} bound for the SST problem under the DST model. (It will be shown later that the same result also holds under the SST model.) Observe that MSAE_{CR}^{S} is symmetric with respect to σ_E, σ_H. It is also independent of whether σ_H and σ_E are known or unknown, as can be shown from Theorem 65.2 and [1, Appendix D]. Also, MSAE_{CR}^{S} is not a function of θ_1, θ_2, θ_3, since for vector sensor measurements the MSAE bound is invariant under rotational transformations of the reference coordinate system. On the other hand, MSAE_{CR}^{S} is influenced by the ellipticity angle θ_4 through the difference in the electric and magnetic noise variances.

Table 65.1 summarizes several special cases of the expression (65.34) for MSAE_{CR}^{S}. The elliptical polarization column corresponds to an arbitrary polarization angle $\theta_4 \in [-\pi/4, \pi/4]$. The circular and linear polarization columns are obtained, respectively, as special cases of Eq. (65.34) with $|\theta_4| = \pi/4$ and $\theta_4 = 0$. The row of precise (noise-free) electric measurement (with noisy magnetic measurements) is obtained by substituting $\sigma_E^2 = 0$ in (65.34). The row of electric measurement only is obtained by deriving the corresponding CRB and MSAE_{CR}^{S}. Alternatively, MSAE_{CR}^{S} can be found for this case by taking the limit of Eq. (65.34) as $\sigma_H^2 \to \infty$.

Observe from Eq. (65.34) that when $\sigma_H^2 \neq \sigma_E^2$, MSAE_{CR}^{S} is minimized for circular polarization and maximized for linear polarization. This result is illustrated in Fig. 65.3, which shows the square root of MSAE_{CR}^{S} as a function of $r = \sigma_H/\sigma_E$ for three types of polarizations ($\theta_4 = 0, \pi/12, \pi/4$). The equivalent signal-to-noise ratio $\mathrm{SNR} = \sigma_s^2/\sigma_{\|}^2$ is kept at one, while the individual electric and magnetic noise variances are varied to give the desired value of r. As r becomes larger or smaller than one, MSAE_{CR}^{S} increases more significantly for sources with polarization closer to linear.

When the electric (or magnetic) field is measured precisely and the source polarization is circular or elliptical, the MSAE_{CR}^{S} is zero (i.e., no angular error), while for linearly polarized sources it remains positive. In the latter case, the contribution to MSAE_{CR}^{S} stems from the magnetic (or electric) noisy measurement. When only the electric (or magnetic) field is measured, MSAE_{CR}^{S} increases as

TABLE 65.1 MSAE Bounds for a Single Signal Transmission Source

	Elliptical	Circular	Linear
General MSAE_{CR}^{S}	(65.34)	$\frac{2(1+\varrho)}{\varrho^2}$	$\frac{(1+\varrho)(\sigma_E^2+\sigma_H^2)}{2\varrho\sigma_s^2}$
Precise electric measurement	0	0	$\frac{\sigma_H^2}{2\sigma_s^2}$
Electric measurement only	$\frac{\sigma_E^2(\sigma_E^2+\sigma_s^2)}{2\sigma_s^4\sin^2\theta_4\cos^2\theta_4}$	$\frac{2\sigma_E^2(\sigma_E^2+\sigma_s^2)}{\sigma_s^4}$	∞

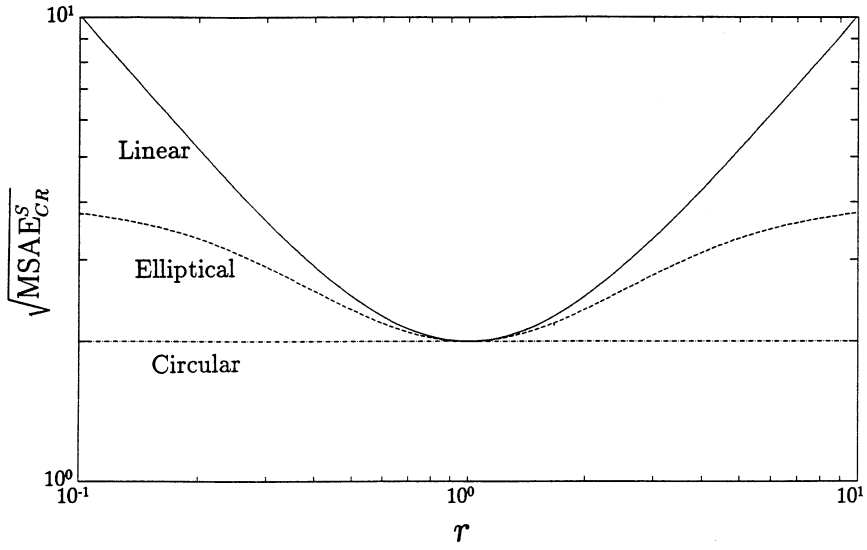

FIGURE 65.3: Effect of change in $r = \sigma_H/\sigma_E$ on MSAE_{CR}^{S} for three types of polarizations ($\theta_4 = 0, \pi/12, \pi/4$). A single SST source, SNR $= \sigma_s^2/\sigma_\parallel^2 = 1$.

the polarization changes from circular to linear. In the linear polarization case, MSAE_{CR}^{S} tends to infinity. In this case, it is impossible to uniquely identify the source direction $\boldsymbol{u}$ from the electric field only, since $\boldsymbol{u}$ can then be anywhere in the plane orthogonal to the electric field vector.

The immediate conclusion is that as the source becomes closer to being linearly polarized it becomes more important to measure both the electric and magnetic fields to get good direction estimates using a single vector sensor.

These results are illustrated in Fig. 65.4, which shows the square root of MSAE_{CR}^{S} as a function of σ_H^2 and three polarization types ($\theta_4 = 0, \pi/12, \pi/4$). The standard deviations of the signal and electric noise are $\sigma_s = \sigma_E = 1$. The left side of the figure corresponds to (nearly) precise magnetic measurement, while the right side to (nearly) electric measurement only.

65.4.4 SST Source (SST Model) Analysis

Suppose that it is desired to estimate the direction to an SST source whose variance is unknown using a single vector sensor, and the estimation is done under the correct model of an SST source. In the following, the CRB for this problem will be derived and it will be shown that the resulting MSAE bound remains the same as when the estimation was done under the assumption of a DST source. That is, knowledge of the source type does not improve the accuracy of its direction estimate.

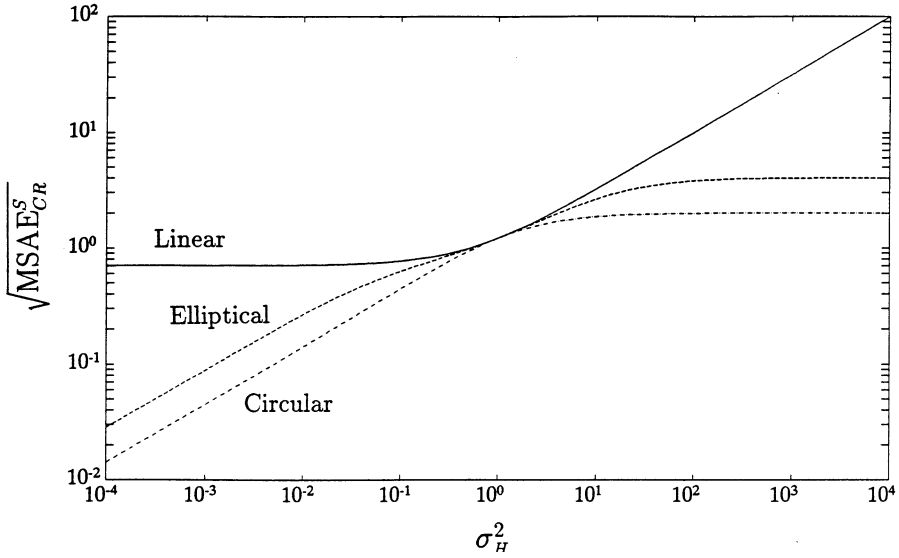

FIGURE 65.4: Effect of change in magnitude of σ_H^2 on MSAE^S_{CR} for three types of polarizations ($\theta_4 = 0, \pi/12, \pi/4$). A single SST source, $\sigma_s = \sigma_E = 1$.

To get a statistical model for the SST measurement model (65.14) as a special case of Eq. (65.21), we will make the same assumptions on the noise and use a similar data scaling as in the above DST source case. That will give again equal noise variances in all the sensor coordinates. Assume also that the signal envelope $s(t)$ satisfies assumption A5 with $x(t) = s(t)$ in Eq. (65.14). Then the resulting statistical model becomes a special case of Eq. (65.21) with

$$\begin{aligned} A &= \begin{bmatrix} rV \\ (\boldsymbol{u}\times)V \end{bmatrix} Q\boldsymbol{w} \qquad x(t) = s(t) \qquad \sigma^2 = \sigma_H^2 \\ \boldsymbol{\theta} &= \begin{bmatrix} \theta_1\,, & \theta_2\,, & \theta_3\,, & \theta_4 \end{bmatrix}^T \end{aligned} \tag{65.35}$$

The unknown parameters are $\boldsymbol{\theta}$, P, σ^2.

The matrix expression of CRB($\boldsymbol{\theta}$) was calculated and its entries are presented in [1, Appendix F]. The results show that the ellipticity angle θ_4 is decoupled from the rest of the parameters and that its variance is not a function of these parameters. Additionally, the parameter vector $\boldsymbol{\theta}$ is decoupled from σ_E and σ_H.

The MSAE bound for an SST source under the SST model was calculated using the analysis of [1]. The result coincides with Eq. (65.34). That is, *the MSAE bound for an SST source is the same under both the SST and the DST models.*

The CRB expression in [1, Appendix F] implies that the CRB variance of the orientation angle θ_3 tends to infinity as the elevation angle θ_2 approaches $\pi/2$ or $-\pi/2$. This singularity is explained by the fact that the orientation angle is a function of the azimuth (through $\boldsymbol{v}_1, \boldsymbol{v}_2$), and the latter becomes increasingly sensitive to measurement errors as the elevation angle approaches the zenith or nadir. (Note that the azimuth is undefined in the zenith and nadir elevations). However, this singularity is not an intrinsic one, as it depends on the chosen reference system, while the information in the vector measurement does not.

65.4.5 CVAE and SST Source Analysis in the Wave Frame

In order to get performance results intrinsic to the SST estimation problem and thereby solve the singularity problems associated with the above model, we choose an alternative error vector that is invariant under known rotational transformations of the coordinate system. The details of the following analysis appear in [1, Appendix G].

Denote by W the wave frame whose coordinate axes are $(\boldsymbol{u}, \widetilde{\boldsymbol{v}}_1, \widetilde{\boldsymbol{v}}_2)$ where $\widetilde{\boldsymbol{v}}_1$ and $\widetilde{\boldsymbol{v}}_2$ correspond, respectively, to the major and minor axes of the source's electric wave ellipse (see Fig. 65.2). For any estimator $\widehat{\theta_i}$, $i = 1, 2, 3$ there is an associated estimated wave frame $\widehat{W}$. Define the vector angular error $\boldsymbol{\phi}_{W\widehat{W}}$ which is the vector angle by which $\widehat{W}$ is (right-handed) rotated about W, and by $\left[\boldsymbol{\phi}_{W\widehat{W}}\right]_W$ the representation of $\boldsymbol{\phi}_{W\widehat{W}}$ in the coordinate system W (see [1, Appendix G]). The proposed vector angular error will be $\left[\boldsymbol{\phi}_{W\widehat{W}}\right]_W$.

Observe that $\left[\boldsymbol{\phi}_{W\widehat{W}}\right]_W$ depends, by definition, only on the frames W, $\widehat{W}$. Thus, for an estimator that is independent of known rotations of the data, the estimated wave frame $\widehat{W}$, the vector angular error and its covariance are independent of the sensor frame. We introduce the following definitions.

DEFINITION 65.4 The *normalized asymptotic covariance of the vector angular error* in the wave frame is defined as

$$\text{CVAE} \triangleq \lim_{N\to\infty} \left\{ N\text{E} \left(\left[\boldsymbol{\phi}_{W\widehat{W}}\right]_W \left[\boldsymbol{\phi}_{W\widehat{W}}\right]_W^T \right) \right\} \tag{65.36}$$

whenever this limit exists.

DEFINITION 65.5 A direction and orientation estimator will be called *regular* if its errors satisfy $\text{E} \sum_{i=1}^{3} |\Delta\theta_i|^3 = o(1/N)$ and the gradient of its bias with respect to $\theta_1, \theta_2, \theta_3$ is $o(1)$ as $N \to \infty$.

Then we have the following theorems.

THEOREM 65.4 *For a regular model the CVAE of any regular direction and orientation estimator, whenever it exists, is bounded from below by*

$$\text{CVAE}_{CR} \triangleq N \cdot K \ \text{CRB}(\theta_1, \theta_2, \theta_3) K^T \tag{65.37}$$

where

$$K = \begin{bmatrix} \sin\theta_2 & 0 & -1 \\ -\cos\theta_2 \sin\theta_3 & -\cos\theta_3 & 0 \\ \cos\theta_2 \cos\theta_3 & -\sin\theta_3 & 0 \end{bmatrix} \tag{65.38}$$

and $\text{CRB}(\theta_1, \theta_2, \theta_3)$ *is the Cramér-Rao submatrix bound for the azimuth, elevation, and orientation angles for the particular model used.*

PROOF 65.4 See [1, Appendix G].

Observe that the result of Theorem 65.4 is obtained using geometrical considerations only. Hence, it is applicable to general direction and orientation estimation problems and is not limited to the SST problem only. It is dependent only on the ability to define a wave frame. For example, one can apply this theorem to a DST source with a wave frame defined by the orientation angle that diagonalizes

the source signal covariance matrix. A generalization of this theorem to estimating non-unit vector systems is given in [26].

For vector sensor measurements, CVAE_{CR} has the desirable property of being invariant to the choice of reference coordinate frame. This invariance property also holds for the CVAE of an estimator if the estimate is independent of deterministic rotational transformations of the data. Note that CVAE_{CR} is not a function of N.

THEOREM 65.5 *The MSAE and CVAE of any regular estimator are related through*

$$\mathrm{MSAE} = [\mathrm{CVAE}]_{2,2} + [\mathrm{CVAE}]_{3,3} \tag{65.39}$$

Furthermore, a similar equality holds for a regular model where the MSAE and CVAE in Eq. (65.39) are replaced by their lower bounds MSAE_{CR} *and* CVAE_{CR}.

PROOF 65.5 See [1, Appendix G].

In our case, $\mathrm{CRB}(\theta_1, \theta_2, \theta_3)$ is the 3×3 upper left block entry of the CRB matrix in the sensor frame given in [1, Appendix F]. Substituting this block entry into Eq. (65.37) and denoting the CVAE matrix bound for the SST problem by CVAE^S_{CR}, we have that this matrix is diagonal with nonzero entries given by

$$\left[\mathrm{CVAE}^S_{CR}\right]_{1,1} = \frac{(1+\varrho)}{2\varrho^2 \cos^2 2\theta_4} \tag{65.40a}$$

$$\left[\mathrm{CVAE}^S_{CR}\right]_{2,2} = \frac{(1+\varrho)(\sigma_E^2+\sigma_H^2)}{2\varrho^2[\sigma_H^2 \sin^2\theta_4 + \sigma_E^2 \cos^2\theta_4]} \tag{65.40b}$$

$$\left[\mathrm{CVAE}^S_{CR}\right]_{3,3} = \frac{(1+\varrho)(\sigma_E^2+\sigma_H^2)}{2\varrho^2[\sigma_E^2 \sin^2\theta_4 + \sigma_H^2 \cos^2\theta_4]} \tag{65.40c}$$

Some observations on Eqs. (65.40) are summarized in the following:

- Rotation around $\boldsymbol{u}$: Singular only for a circularly polarized signal.
- Rotation around $\widetilde{\boldsymbol{v}}_1$ (electric ellipse's major axis): Singular only for a linearly polarized signal and no magnetic measurement.
- Rotation around $\widetilde{\boldsymbol{v}}_2$ (electric ellipse's minor axis): Singular only for a linearly polarized signal and no electric measurement.
- The rotation variances around $\widetilde{\boldsymbol{v}}_1$ and $\widetilde{\boldsymbol{v}}_2$ are symmetric with respect to the electric and magnetic measurements.
- All the three variances in Eq. (65.40) are bounded from below by $(1+\varrho)/2\varrho^{\,2}$ (independent of the wave parameters).

The singular cases above are found by checking when their variances in CVAE^S_{CR} tend to infinity (see, e.g., [25, Theorem 6.3]). The three singular cases above should be expected as the corresponding rotations are unobservable. These singularities are intrinsic to the SST estimation problem and are independent of the reference coordinate system. The symmetry of the variances of the rotations around the major and minor axes of the ellipse with respect to the magnetic and electric measurements should be expected as their axes have a spatial angle difference of $\pi/2$.

The fact that the resulting singularities in the rotational errors are intrinsic (independent of the reference coordinate system) as well as the diagonality of the CVAE_{CR}^{S} bound matrix with its simple entry expressions indicate that the wave frame is a natural system in which to do the analysis.

65.4.6 A Cross-Product-Based DOA Estimator

We propose a simple algorithm for estimating the DOA of a single electromagnetic source using the measurements of a single vector sensor. The motivation for this algorithm stems from the average cross-product Poynting vector. Observe that $-\boldsymbol{u}$ is the unit vector in the direction of the Poynting vector given by [27],

$$\begin{aligned} S(t) &= E(t) \times H(t) = \mathrm{Re}\left\{e^{i\omega_c t}\mathcal{E}(t)\right\} \times \mathrm{Re}\left\{e^{i\omega_c t}\mathcal{H}(t)\right\} \\ &= \tfrac{1}{2}\mathrm{Re}\left\{\mathcal{E}(t) \times \overline{\mathcal{H}}(t)\right\} + \tfrac{1}{2}\mathrm{Re}\left\{e^{i2\omega_c t}\mathcal{E}(t) \times \mathcal{H}(t)\right\} \end{aligned}$$

where $\overline{\mathcal{H}}$ denotes the complex conjugate of $\mathcal{H}$. The carrier time average of the Poynting vector is defined as $\langle S\rangle_t \triangleq \frac{1}{2}\mathrm{Re}\{\mathcal{E}(t) \times \overline{\mathcal{H}}(t)\}$. Note that unlike $\mathcal{E}(t)$ and $\mathcal{H}(t)$ this average is not a function of ω_c. Thus, it has an intrinsic physical meaning.

At this point we can see two possible ways for estimating $\boldsymbol{u}$:

1. Phasor time averaging of $\langle S\rangle_t$ yielding a vector denoted by $\langle S\rangle$ with the estimated $\boldsymbol{u}$ taken as the unit vector in the direction of $-\langle S\rangle$.
2. Estimation of $\boldsymbol{u}$ by phasor time averaging of the unit vectors in the direction of $\mathrm{Re}\{\mathcal{E}(t) \times \overline{\mathcal{H}}(t)\}$.

Clearly, the first way is preferable, since then $\boldsymbol{u}$ is estimated after the measurement noise is reduced by the averaging process, while the estimated $\boldsymbol{u}$ in the second way is more sensitive to the measurement noises which may be magnified considerably.

Thus, the proposed algorithm computes

$$\widehat{\boldsymbol{s}} = \frac{1}{N}\sum_{t=1}^{N}\mathrm{Re}\{\boldsymbol{y}_E(t) \times \overline{\boldsymbol{y}}_H(t)\} \tag{65.41a}$$

$$\widehat{\boldsymbol{u}} = \widehat{\boldsymbol{s}}/\|\widehat{\boldsymbol{s}}\| \tag{65.41b}$$

This algorithm and some of its variants have been patented [28].

The statistical performance of this estimator $\widehat{\boldsymbol{u}}$ is analyzed in [1, Appendix H] under the previous assumptions on $\boldsymbol{\xi}(t)$, $\boldsymbol{e}_E(t)$, $\boldsymbol{e}_H(t)$, except that the Gaussian assumption is omitted. The results are summarized by the following theorem.

THEOREM 65.6 *The estimator $\widehat{\boldsymbol{u}}$ has the following properties (for both* DST *and* SST *sources):*

a) If $\|\boldsymbol{\xi}(t)\|^2$, $\|\boldsymbol{e}_E(t)\|$, $\|\boldsymbol{e}_H(t)\|$ have finite first order moments, then $\widehat{\boldsymbol{u}} \to \boldsymbol{u}$ almost surely.

b) If $\|\boldsymbol{\xi}(t)\|^2$, $\|\boldsymbol{e}_E(t)\|$, $\|\boldsymbol{e}_H(t)\|$ have finite second order moments, then $\sqrt{N}(\widehat{\boldsymbol{u}} - \boldsymbol{u})$ is asymptotically normal.

c) If $\|\boldsymbol{\xi}(t)\|^2$, $\|\boldsymbol{e}_E(t)\|$, $\|\boldsymbol{e}_H(t)\|$ have finite fourth order moments, then the MSAE *is*

$$\mathrm{MSAE} = \tfrac{1}{2}\varrho^{-1}\left(1 + 4\varrho^{-1}\right)\left(r + r^{-1}\right)^2 \tag{65.42}$$

where $\varrho = \mathrm{tr}\,(P)/\sigma_{\|}^2$ = SNR.

d) Under the conditions of (c), $N\delta^2$ is asymptotically χ^2 distributed with two degrees of freedom.

PROOF 65.6 See [1, Appendix H].

For the Gaussian SST case, the ratio between the MSAE of this estimator to MSAE_{CR}^{S} in Eq. (65.34) is

$$\text{eff} \triangleq \frac{\text{MSAE}}{\text{MSAE}_{CR}^{S}} = \frac{\varrho+4}{\varrho+1}\left[1+(r-r^{-1})^2\sin^2\theta_4\cos^2\theta_4\right] \tag{65.43}$$

Hence, this estimator is nearly efficient if the following two conditions are met:

$$\varrho \gg 1 \tag{65.44a}$$

$$r \simeq 1 \quad \text{or} \quad \theta_4 \simeq 0 \tag{65.44b}$$

Figure 65.5 illustrates these results using plots of the efficiency factor (65.43) as a function of the ellipticity angle θ_4 for SNR $= \varrho = 10$ and three different values of r.

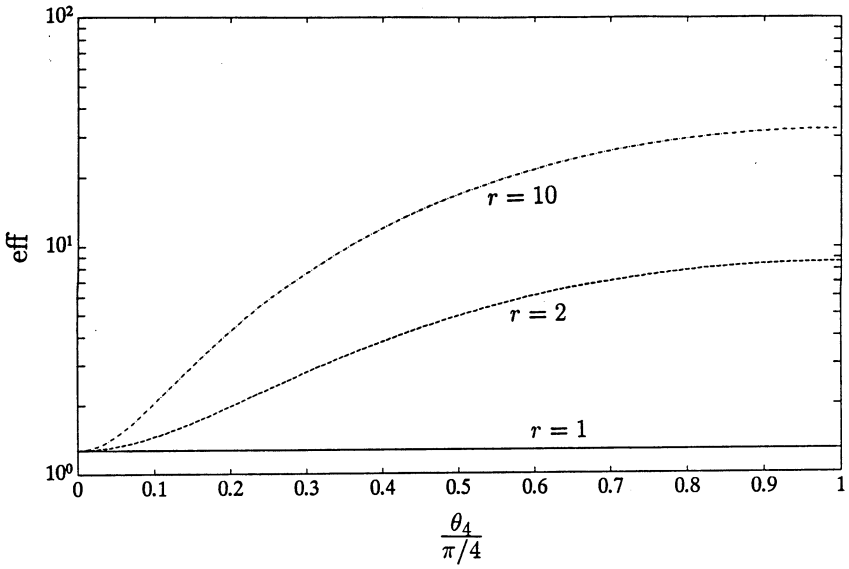

FIGURE 65.5: The efficiency factor (65.43) of the cross-product-based direction estimator as a function of the normalized ellipticity angle for three values of $r = \sigma_H/\sigma_E$. A single source, SNR $= 10$.

The estimator (65.41) can be improved using a weighted average of cross products between all possible pairs of real and imaginary parts of $\boldsymbol{y}_E(t)$ and $\boldsymbol{y}_H(s)$ taken at arbitrary times t and s. (Note that these cross products have directions nearly parallel to the basic estimator $\widehat{\boldsymbol{u}}$ in Eq. (65.41); however, before averaging, these cross products should be premultiplied by $+1$ or -1 in accordance with the direction of the basic estimator $\widehat{\boldsymbol{u}}$). A similar algorithm suitable for real time applications can also be developed in the time domain without preprocessing needed for phasor representation. It can be extended to nonstationary inputs by using a moving average window on the data. It is of

interest to find the optimal weights and the performances of these estimators.

The main advantages of the proposed cross-product-based algorithm (65.41) or one of its variants above are

- It can give a direction estimate instantly, i.e., with one time sample.
- It is simple to implement (does not require minimization of a cost function) and can be applied in real time.
- It is equally applicable to sources of various types, including SST, DST, wide-band, and non-Gaussian.
- Its MSAE is nearly optimal in the Gaussian SST case under Eq. (65.44).
- It does not depend on time delays and therefore does not require data synchronization among different sensor components.

65.5 Multi-Source Multi-Vector Sensor Analysis

Consider the case in which it is desired to estimate the directions to multiple electromagnetic sources whose covariance is unknown using an array of vector sensors. The MSAE_{CR} and CVAE_{CR} bound expressions in Eqs. (65.29) and (65.37) are applicable to each of the sources in the multi-source multi-vector sensor scenario. Suppose that the noise vector $\boldsymbol{e}_{EH}(t)$ in Eq. (65.19) is complex white Gaussian with zero mean and diagonal covariance matrix (i.e., noises from different sensors are uncorrelated) and with electric and magnetic variances σ_E^2 and σ_H^2, respectively. Suppose also that $r = \sigma_H/\sigma_E$ is known. Similarly to the single sensor case, multiply the electric measurements in Eq. (65.19) by r to obtain equal noise variances in all the sensor coordintates. The resulting models then become special cases of Eq. (65.21) as follows.

For DST signals, the block columns $A_k \in \mathbb{C}^{6m\times 2}$ and the signals $\boldsymbol{x}(t) \in \mathbb{C}^{2n\times 1}$ are

$$A_k = \boldsymbol{e}_k \otimes \begin{bmatrix} r\,I_3 \\ (\boldsymbol{u}_k\times) \end{bmatrix} V_k \tag{65.45a}$$

$$\boldsymbol{x}(t) = \left[\boldsymbol{\xi}_1^T(t),\ \cdots,\ \boldsymbol{\xi}_n^T(t)\right]^T \tag{65.45b}$$

The parameter vector of the kth source includes here its azimuth and elevation.

For the SST case, the columns $A_k \in \mathbb{C}^{6m\times 1}$ and the signals $\boldsymbol{x}(t) \in \mathbb{C}^{n\times 1}$ are

$$A_k = \boldsymbol{e}_k \otimes \begin{bmatrix} r\,I_3 \\ (\boldsymbol{u}_k\times) \end{bmatrix} V_k Q_k \boldsymbol{w}_k \tag{65.46a}$$

$$\boldsymbol{x}(t) = [s_1(t),\ \cdots,\ s_n(t)]^T \tag{65.46b}$$

The parameter vector of the kth source includes here its azimuth, elevation, orientation, and ellipticity angles.

The matrices A whose (block) columns are given in Eqs. (65.45a) and (65.46a) are the Khatri-Rao products (see, e.g., [20, 21]) of the two matrices whose (block) columns are the arguments of the Kronecker products in these equations.

Mixed single and dual signal transmissions are also special cases of Eq. (65.21) with appropriate combinations of the above expressions.

65.5.1 Results for Multiple Sources, Single-Vector Sensor

We present several results for the multiple-source model and a single-vector sensor. It is assumed that the signal and noise vectors satisfy, respectively, assumptions A5 and A6. The results are applicable to wide-band sources since a single vector sensor is used and thus A3 and A4 are not needed.

We first present results obtained by numerical evaluation concerning the localization of *two* uncorrelated sources, assuming r is known:

1. When only the electric field is measured, the information matrix is singular.
2. When the electric measurement is precise, the CRB variances are generally nonzero.
3. The MSAE^S_{CR} can increase without bound with decreasing source angular separation for sources with the same ellipticity and spin direction, but remarkably it remains bounded for sources with different ellipticities or opposite spin directions.

Properties 1 and 2 are, in general, different from the single source case. Property 1 shows that it is necessary to include both the electric and magnetic measurements to estimate the direction to more than one source. Property 3 demonstrates the great advantage of using the electromagnetic vector sensor, in that it allows high resolution of sources with different ellipticities or opposite spins. Note that this generally requires a very large aperture using a scalar sensor array.

The above result on the ability to resolve two sources that are different only in their ellipticity or spin direction appears to be new. Note also the analogy to Pauli's "exclusion principle", as in our case two narrow-band SST sources are distinguishable if and only if they have different sets of parameters. The set in our case includes wave-length, direction, ellipticity, and spin sign.

Now we present conditions for identifiability of multiple SST (or polarized) sources and a single vector sensor, which are analytically proven in [29] and [30], assuming the noise variances are known:

1. A single source is always identifiable.
2. Two sources that are not fully correlated are identifiable if they have different DOAs.
3. Two fully correlated sources are identifiable if they have different DOAs and ellipticities.
4. Three sources that are not fully correlated are identifiable if they have different DOAs and ellipticities.

Note that by identifiability we refer to both the DOA and polarization parameters.

Figures 65.6 and 65.7 illustrate the resolution of two uncorrelated equal power SST sources with a single electromagnetic vector sensor. The figures show the square root of the MSAE^S_{CR} of one of the sources for a variety of spin directions, ellipticities, and orientation angles, as a function of the separation angle between the sources. (The MSAE^S_{CR} values of the two sources are found to be equal in all the following cases.) The covariances of the signals and noise are normalized such that $P = I_2, \sigma_E = \sigma_H = 1$. The azimuth angle of the first source and the elevation angles of the two sources are kept constant ($\theta_1^{(1)} = \theta_2^{(1)} = \theta_2^{(2)} = 0$). The second source's azimuth is varied to give the desired separation angle $\Delta\theta_1$, $\theta_1^{(2)}$. In Fig. 65.6, the cases shown are of same spin directions ($\theta_4^{(1)} = \theta_4^{(2)} = \pi/12$) and opposite spin directions ($\theta_4^{(1)} = -\theta_4^{(2)} = \pi/12$), same orientation angles ($\theta_3^{(1)} = \theta_3^{(2)} = \pi/4$) and different orientation angles ($\theta_3^{(1)} = -\theta_3^{(2)} = \pi/4$). The figure shows that the resolution of the two sources with a single vector sensor is remarkably good when the sources have opposite spin directions. In particular, the MSAE^S_{CR} remains bounded even for zero separation angle and equal orientation angles! On the other hand, the resolution is not so significant when the two sources have different orientation angles but equal ellipticity angles (then, for example, the MSAE^S_{CR} tends to infinity for zero separation angle). In Fig. 65.7, the orientation angles of the sources is the same ($\theta_3^{(1)} = \theta_3^{(2)} = \pi/4$), the polarization of the first source is kept linear ($\theta_4^{(1)} = 0$) while the

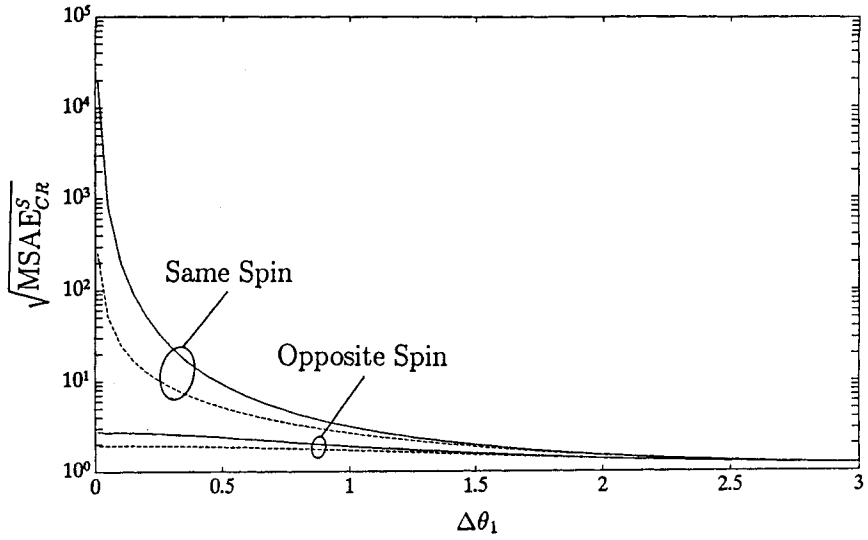

FIGURE 65.6: MSAE^S_{CR} for two uncorrelated equal power SST sources and a single vector sensor as a function of the source angular separation. Upper two curves: Same spin directions ($\theta_4^{(1)} = \theta_4^{(2)} = \pi/12$). Lower two curves: Opposite spin directions ($\theta_4^{(1)} = -\theta_4^{(2)} = \pi/12$). Solid curves: Same orientation angles ($\theta_3^{(1)} = \theta_3^{(2)} = \pi/4$). Dashed curves: Different orientation angles ($\theta_3^{(1)} = -\theta_3^{(2)} = \pi/4$). Remaining parameters are $\theta_1^{(1)} = \theta_2^{(1)} = \theta_2^{(2)} = 0$, $\Delta\theta_1 \triangleq \theta_1^{(2)}$, $P = I_2$, $\sigma_E = \sigma_H = 1$.

ellipticity angle of the second source is varied ($|\theta_4^{(2)}| = \pi/12,\ \pi/6,\ \pi/4$) to illustrate the remarkable resolvability due to different ellipticities. It can be seen that the MSAE^S_{CR} remains bounded here even for zero separation angle.

Thus, Figs. 65.6 and 65.7 show that with one vector sensor it is possible to resolve extremely well two uncorrelated SST sources that have only different spin directions or different ellipticities (these sources can have the same direction of arrival and the same orientation angle). This demonstrates a great advantage of the vector sensor over scalar sensor arrays, in that the latter require large array apertures to resolve sources with small separation angle.

65.6 Concluding Remarks

An approach has been presented for the localization of electromagnetic sources using vector sensors. We summarize some of the main results of this article and give an outlook to their possible extensions.

Models: New models that include the complete electromagnetic data at each sensor have been introduced. Furthermore, new signal models and vector angular error models in the wave frame have been proposed. The wave frame model provides simple performance expressions that are easy to interpret and have only intrinsic singularities. Extensions of the proposed models may include additional structures for specific applications.

Cramér-Rao bounds and quality measures: A compact expression for the CRB for multi-vector source multi-vector sensor processing has been derived. The derivation gave rise to new block matrix operators. New quality measures in three-dimensional space, such as the MSAE for direction estimation and CVAE for direction and orientation estimation, have been defined. Explicit bounds on the MSAE and CVAE, having the desirable property of being invariant to the choice of the

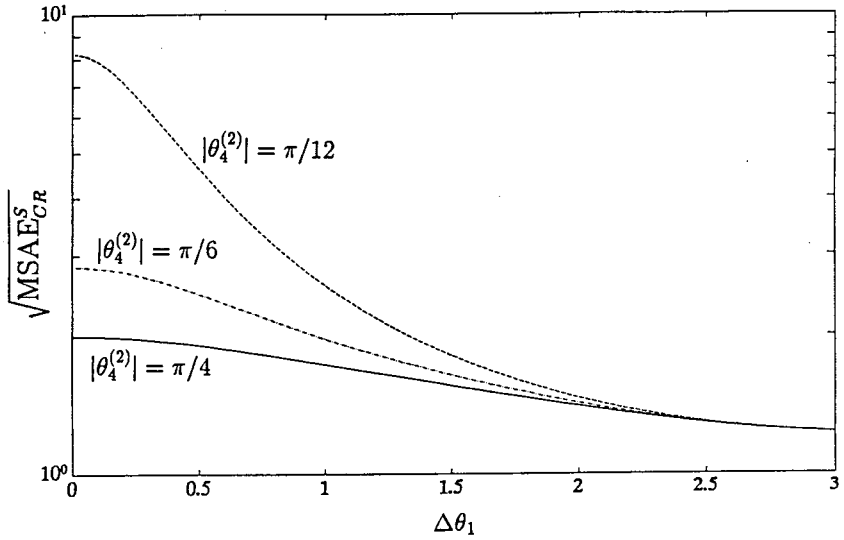

FIGURE 65.7: MSAE^S_{CR} for two uncorrelated equal power SST sources and a single vector sensor as a function of the source angular separation. Sources are with the same orientation angles ($\theta_3^{(1)} = \theta_3^{(2)} = \pi/4$) and different ellipticity angles ($\theta_4^{(1)} = 0$ and $\theta_4^{(2)}$ as shown in the figure). Remaining parameters are as in Fig. 65.6.

reference coordinate frame, have been derived and can be used for performance analysis. Some generalizations of the bounds appear in [26]. These bounds are not limited to electromagnetic vector sensor processing. Performance comparisons of vector sensor processing with scalar sensor counterparts are of interest.

Identifiablity: The derived bounds and the identifiability analysis of [29] and [30] were used to show that the fusion of magnetic and electric data at a single vector sensor increases the number of identifiable sources (or resolution capacity) in three-dimensional space from one source in the electric data case to up to three sources in the electromagnetic case. For a single signal transmission source, in order to get good direction estimates, the fusion of the complete data becomes more important as the polarization gets closer to linear. Finding the number of identifiable sources per sensor in a general vector sensor array is of interest. Preliminary results on this issue can be found in [29, 31].

Resolution: Source resolution using vector sensors is inherently different from scalar sensors, where the latter case is characterized by the classical Rayleigh principle. For example, it was shown that a single vector sensor can be used to resolve two sources in three-dimensional space. In particular, a vector sensor exhibits remarkable resolvability when the sources have opposite spin directions or different ellipticity angles. This is very different from the scalar sensor array case in which a plane array with large aperture is required to achieve the same goal. Analytical results on source resolution using vector sensor arrays and comparisons with their scalar counterparts are of interest.

Algorithms: A simple algorithm has been proposed and analyzed for finding the direction to a single source using a single vector sensor based on the cross-product operation. It is of interest to analyze the performance of the aformentioned variants of this algorithm and to extend them to more general source scenarios (e.g., larger number of sources). It is also of interest to develop new algorithms for the vector sensor array case.

Communication: The main considerations in communication are transmission of signals over channels with limited bandwidth and their recovery at the sensor. Vector sensors naturally fit these

considerations as they have maximum observability to incoming signals and they double the channel capacity (compared with scalar sensors) with DST signals. This has vast potential for performance improvement in cellular communications. Future goals will include development of optimum signal estimation algorithms, communication forms, and coding design with vector-sensor arrays.

Implementations: The proposed methods should be implemented and tested with real data.

Sensor development: The use of complete electromagnetic data seemes to be virtually nonexistant in the literature on source localization. It is hoped that the results of this research will motivate the systematic development of high quality electromagnetic sensors that can operate over a broad range of frequencies. Recent references on this topic can be found in [14] and [15].

Extensions: The vector sensor concept can be extended to other areas and open new possibilities. An example of this can be found in [32] and [33] for the acoustic case.

Acknowledgment

The authors are grateful to Professor I.Y. Bar-Itzhack from the Department of Aeronautical Engineering, Technion, Israel, for bringing reference [34] to their attention.

References

[1] Nehorai, A. and Paldi, E., Vector-sensor array processing for electromagnetic source localization, *IEEE Trans. on Signal Processing*, SP-42, 376–398, Feb. 1994.

[2] Nehorai, A. and Paldi, E., Vector sensor processing for electromagnetic source localization, *Proc. 25th Asilomar Conf. Signals, Syst. Comput.*, Pacific Grove, CA, Nov. 1991, 566–572.

[3] Schwartz, M., Bennett, W.R. and Stein, S., *Communication Systems and Techniques*, McGraw-Hill, New York, 1966.

[4] Keiser, B.E., *Broadband Coding, Modulation, and Transmission Engineering*, Prentice-Hall, Englewood Cliffs, New Jersey, 1989.

[5] Stoica, P. and Nehorai, A., Performance study of conditional and unconditional direction-of-arrival estimation, *IEEE Trans. Acoust., Speech, Signal Processing*, ASSP-38, 1783–1795, Oct. 1990.

[6] Ottersten, B., Viberg, M. and Kailath, T., Analysis of subspace fitting and ML techniques for parameter estimation from sensor array data, *IEEE Trans. Signal Processing*, SP-40, 590–600, March 1992.

[7] Schmidt, R.O., A signal subspace approach to multiple emitter location and spectral estimation, Ph.D., Dissertation, Stanford University, Stanford, CA, Nov. 1981.

[8] Ferrara, Jr., E.R. and Parks, T.M., Direction finding with an array of antennas having diverse polarization, *IEEE Trans. Antennas Propagat.*, AP-31, 231–236, March 1983.

[9] Ziskind, I. and Wax, M., Maximum likelihood localization of diversely polarized sources by simulated annealing, *IEEE Trans. Antennas Propagat.*, AP-38, 1111–1114, July 1990.

[10] Li, J. and Compton, R.T., Jr., Angle and polarization estimation using ESPRIT with a polarization sensitive array, *IEEE Trans. Antennas Propagat.*, AP-39, 1376–1383, Sept. 1991.

[11] Weiss, A.J. and Friedlander, B., Performance analysis of diversely polarized antenna arrays, *IEEE Trans. Signal Processing*, SP-39, 1589–1603, July 1991.

[12] Means, J.D., Use of three-dimensional covariance matrix in analyzing the polarization properties of plane waves, *J. Geophys. Res.*, 77, 5551–5559, Oct. 1972.

[13] Hatke, G.F., Performance analysis of the SuperCART antenna array, Project Report No. AST-22, Lincoln Laboratory, Massachusetts Institute of Technology, Lexington, MA, March 1992.

[14] Kanda, M., An electromagnetic near-field sensor for simultaneous electric and magnetic-field measurements, *IEEE Trans. on Electromagnetic Compatibility*, 26(1), 102–110, Aug. 1984.

[15] Kanda, M. and Hill, D., A three-loop method for determining the radiation characteristics of an electrically small source, *IEEE Trans. on Electromagnetic Compatibility*, 34(1), 1–3, Feb. 1992.
[16] Dugundji, J., Envelopes and pre-envelopes of real waveforms, *IRE Trans. Information Theory*, IT-4, 53–57, March 1958.
[17] Rice, S.O., Envelopes of narrow-band signals, *Proc. IEEE*, 70, 692–699, July 1982.
[18] Giuli, D., Polarization diversity in radars, *Proc. IEEE*, 74, 245–269, Feb. 1986.
[19] Born, M. and Wolf, E., Eds., *Principles of Optics*, 6th ed., Pergamon Press, Oxford, 1980 [1st ed., 1959].
[20] Khatri, C.G. and Rao, C.R., Solution to some functional equations and their applications to characterization of probability distribution, *Sankhyā Ser. A*, 30, 167–180, 1968.
[21] Rao, C.R. and Mitra, S.K., *Generalized Inverse of Matrices and its Applications*, John Wiley & Sons, New York, 1971.
[22] Stoica, P. and Nehorai, A., MUSIC, maximum likelihood and Cramér-Rao bound, *IEEE Trans. Acoust., Speech, Signal Processing*, ASSP-37, 720–741, May 1989.
[23] Ibragimov, I.A. and Has'minskii, R.Z., *Statistical Estimation: Asymptotic Theory*, Springer-Verlag, New York, 1981.
[24] Paldi, E. and Nehorai, A., A generalized Cramér-Rao bound, in preparation.
[25] Caines, P.E., *Linear Stochastic Systems*, John Wiley & Sons, New York, 1988.
[26] Nehorai, A. and Hawkes, M., Performance bounds on estimating vector systems, in preparation.
[27] Jackson, J.D., *Classical Electrodynamics*, 2nd ed., John Wiley & Sons, New York, 1975 [1st ed., 1962].
[28] Nehorai, A. and Paldi, E., Method for electromagnetic source localization, U.S. Patent No. 5,315,308, May 24, 1994.
[29] Hochwald, B. and Nehorai, A., Identifiability in array processing models with vector-sensor applications, *IEEE Trans. Signal Process.*, SP-44, 83–95, Jan. 1996.
[30] Ho, K.-C., Tan, K.-C. and Ser, W., An investigation on number of signals whose direction-of-arrival are uniquely determinable with an electromagnetic vector sensor, *Signal Processing*, 47, 41–54, Nov. 1995.
[31] Tan, K.-C., Ho, K.-C. and Nehorai, A., Uniqueness study of measurements obtainable with arrays of electromagnetic vector sensors, *IEEE Trans. Signal Process.*, SP-44, 1036–1039, Apr. 1996.
[32] Nehorai, A. and Paldi, E., Acoustic vector-sensor array processing, *IEEE Trans. on Signal Processing*, SP-42, 2481–2491, Sept. 1994. A short version appeared in *Proc. 26th Asilomar Conf. Signals, Syst. Comput.*, Pacific Grove, CA, Oct. 1992, 192–198.
[33] Hawkes, M. and Nehorai, A., Acoustic vector-sensor beamforming and capon direction estimation, *IEEE Int. Conf. Acoust., Speech, Signal Processing*, Detroit, MI, May 1995, 1673–1676.
[34] Shuster, M.D., A Survey of attitude representations, *J. Astronaut. Sci.*, 41(4), 439–517, Oct.–Dec. 1993.

Appendix A: Definitions of Some Block Matrix Operators

This appendix defines several block matrix operators that are found to be useful in this article. The following notation will be used for a blockwise partitioned matrix A:

$$A = \begin{bmatrix} A_{<11>} & \cdots & A_{<1n>} \\ \vdots & & \vdots \\ A_{<m1>} & \cdots & A_{<mn>} \end{bmatrix} \triangleq \left[A_{<ij>} \right] \tag{A.1}$$

with the block entries $A_{<ij>}$ of dimensions $\mu_i \times \nu_j$. Define $\overline{\mu} \triangleq \sum_{i=1}^{m} \mu_i$, $\overline{\nu} \triangleq \sum_{j=1}^{n} \nu_j$, so A is a $\overline{\mu} \times \overline{\nu}$ matrix. Since the block entries may not be of the same size, this is sometimes called an unbalanced partitioning. The following definitions will be considered.

DEFINITION 65.6 *Block transpose.* Let A be an $m\mu \times n\nu$ blockwise partitioned matrix, with blocks $A_{<ij>}$ of equal dimensions $\mu \times \nu$. Then the block transpose A^{bT} is an $n\mu \times m\nu$ matrix defined through

$$\left(A^{bT}\right)_{<ij>} = A_{<ji>} \tag{A.2}$$

DEFINITION 65.7 *Block Kronecker product.* Let A be a blockwise partitioned matrix of dimension $\overline{\mu} \times \overline{\nu}$, with block entries $A_{<ij>}$ of dimensions $\mu_i \times \nu_j$, and let B be a blockwise partitioned matrix of dimensions $\overline{\eta} \times \overline{\rho}$, with block entries $B_{<ij>}$ of dimensions $\eta_i \times \rho_j$. Also $\overline{\mu} = \sum_{i=1}^{m} \mu_i$, $\overline{\nu} = \sum_{j=1}^{n} \nu_j$, $\overline{\eta} = \sum_{i=1}^{m} \eta_i$, $\overline{\rho} = \sum_{j=1}^{n} \rho_j$. Then the block Kronecker product $A \boxtimes B$ is an $(\sum_{i=1}^{m} \mu_i \eta_i \times \sum_{j=1}^{n} \nu_j \rho_j)$ matrix defined through

$$(A \boxtimes B)_{<ij>} = A_{<ij>} \otimes B_{<ij>} \tag{A.3}$$

i.e., the (i, j) block entry of $A \boxtimes B$ is $A_{<ij>} \otimes B_{<ij>}$ of dimension $\mu_i \eta_i \times \nu_j \rho_j$.

DEFINITION 65.8 *Block Schur-Hadamard product.* Let A be an $m\mu \times n\nu$ matrix consisting of blocks $A_{<ij>}$ of dimensions $\mu \times \nu$, and let B be an $m\nu \times n\eta$ matrix consisting of blocks $B_{<ij>}$ of dimensions $\nu \times \eta$. Then the block Schur-Hadamard product $A \boxdot B$ is an $m\mu \times n\eta$ matrix defined through

$$(A \boxdot B)_{<ij>} = A_{<ij>} B_{<ij>} \tag{A.4}$$

Thus, each block of the product is a *usual* product of a pair of blocks and is of dimension $\mu \times \eta$.

DEFINITION 65.9 *Block trace operator.* Let A be an $m\mu \times n\mu$ matrix consisting of blocks $A_{<ij>}$ of dimensions $\mu \times \mu$. Then the block trace matrix operator btr$[A]$ is an $m \times n$ matrix defined by

$$(\text{btr}\,[A])_{ij} = \text{tr}\; A_{<ij>} \tag{A.5}$$